Special Issue Article

Advances in Mechanical Engineering

Advances in Mechanical Engineering
2017, Vol. 9(8) 1–13

DOI: 10.1177/1687814017701703
journals.sagepub.com/home/ade
SAGE

Modeling and analyses of a connected multi-car train system employing the inerter

Hsueh-Ju Chen[1,2], Wei-Jiun Su[1] and Fu-Cheng Wang[1]

Abstract

This article develops the model of a connected multi-car train system and discusses the improvement of stability and performance by the inerter. The inerter is a genuine two-terminal element, whose reacting force is proportional to the relative acceleration across its terminals. First, we build a 31-degree-of-freedom full-train model by a multi-body package, called AutoSim, and show that its stability can be significantly improved by the inerter. Second, we derive a multi-car train model, by another multi-body package, called SimMechanics, and discuss the impacts of the number of connected cars on system stability: connecting cars tends to decrease the critical speed. Furthermore, we extend the discussion to performance and show that the connecting cars will increase the settling time, but has no influence on the passenger comfort. Finally, we apply network synthesis methods to realize a mechatronic network and conduct experimental verification. Based on the results, the inerter is deemed effective in improving the stability and performance of connected multi-car trains.

Keywords

Multi-car trains, critical speed, performance, inerter, network synthesis, AutoSim, SimMechanics

Date received: 4 September 2016; accepted: 6 February 2017

Academic Editor: Xiaoting Rui

Introduction

Analogies between mechanical and electrical systems have drawn much attention and led to the invention of the inerter.[1] The inerter is proposed to be the substitute for the mass element, with the reacting force proportional to the relative acceleration of its two terminals. The introduction of the inerter lets mechanical networks become truly analogous to electrical ones. Consequently, all passive mechanical networks can be constructed by inerters, dampers, and springs, and the performance of mechanical systems can now be improved passively (i.e. without consuming extra energy). There are several mechanical realizations of inerter, including the rack-pinion inerter,[2] the ball-screw inerter,[3] the hydraulic inerter,[4] and the mechatronic network.[5] Among these, the first three are pure mechanical constructions, whereas the fourth consists of a ball-screw inerter and a motor generator so that the system impedance/admittance can be easily adjusted by the electrical networks.

The inerter has been successfully applied to vehicle suspensions,[2] motorcycle steering,[6] and building models.[7] The results confirmed the significant improvement on system stability and performance by implementing the inerter. Many studies have also discussed

[1]Department of Mechanical Engineering, National Taiwan University, Taipei, Taiwan
[2]School of Electrical and Electronic Engineering, University of Manchester, Manchester, UK

Corresponding author:
Fu-Cheng Wang, Department of Mechanical Engineering, National Taiwan University, No.1, Section 4, Roosevelt Road, Taipei 10617, Taiwan.
Email: fcw@ntu.edu.tw

the stability and performance of train systems employing the inerter. For example, Wang and Liao[8] discussed the stability of a 16-degree-of-freedom (DOF) train model. Wang et al.[9] further considered the performance improvement of the train model with the inerter. Jiang et al.[10] investigated the lateral passenger comfort. The effects of inter-vehicle connections are studied based on multi-body dynamics theory. For instance, Ling et al.[11] discussed the impacts of vehicle connections on the dynamic behavior of train models. They compared the dynamic performances of the single-car and the multi-car train models without the inerter. This article extends the discussion to train models with the inerter. We built the single-car and multi-car train models in AutoSim and SimMechanics, respectively. Because there has been no profound discussion on how connected cars might influence system stability and performance using inerters, in this article, we apply the models to discuss how the number of connected cars could influence the stability and performance of trains employing inerters.

The main contributions of this article are as follows: we developed a 31-DOF full-train model that included the pitch motions of the car body and bogies, and we constructed multi-car train models to investigate the impacts of connecting cars on stability and performance of the system employing the inerter. This article is arranged as follows: in section "The 31-DOF full-train model," we derive a 31-DOF full-train model. We then apply seven suspension layouts to discuss how the model stability can be improved by the inerter. Section "Connected multi-car train model" derives multi-car train models and discusses the impacts of connecting cars on the critical speed, settling time, and passenger comfort. Section "Network synthesis" realizes an optimal electrical circuit and conducts experimental verification. Finally, we draw conclusions in section "Conclusion."

The 31-DOF full-train model

The full-train model is shown in Figure 1, which consists of a car body, two bogies, and four wheel-sets. We assume a constant forward velocity and neglect the longitudinal (x-direction) motions, and derive a full-train model that has 31 DOFs (see Table 1) with the default parameters as illustrated in Table 2. The full-train model consists of two main suspensions. The primary suspension is between the bogie and the wheel-sets, denoted Q_{px}, Q_{py}, and Q_{pz} in the x-, y-, and z-direction, respectively. The secondary suspension is between the car body and the bogie, denoted as Q_{sx}, Q_{sy}, and Q_{sz} in the x-, y-, and z-direction, respectively.

The dynamic equations of the full-train model are shown in Appendix 1. We also build the full-train model by a multi-body package, called AutoSim (see Appendix 2), for model verification. We derive the following linearized hand-derivation model (G_H) and AutoSim model (G_A) for comparison

$$G_H = \left[\begin{array}{c|c} A_H & B_H \\ \hline C_H & D_H \end{array}\right] = \begin{cases} \dot{x} = A_H x + B_H u \\ y = C_H x + D_H u \end{cases},$$
$$G_A = \left[\begin{array}{c|c} A_A & B_A \\ \hline C_A & D_A \end{array}\right] = \begin{cases} \dot{x} = A_A x + B_A u \\ y = C_A x + D_A u \end{cases}$$

We compare the elements, eigenvalues, and singular values of the two system matrices (A_H and A_A), and confirm that the two models are the same. Therefore, we can use the model for stability and performance analysis in section "Connected multi-car train model."

Suspension layouts employing the inerter

The dynamics of an inerter is as follows[1]

$$F = b \cdot a = b \cdot \frac{d^2x}{dt^2}$$

where F is the reacting force, a is the relative acceleration between two terminals, b is the inertance (kg), and x is the relative displacement between two terminals. However, the mechatronic network (see Figure 2(a)) consists of a ball-screw inerter and a permanent magnet electric machinery (PMEM) with an electrical circuit, such that the system admittance is a combination of mechanical and electrical systems as follows[5]

$$Y_{ms} = \frac{F(s)}{v(s)} = b_m s + c_m + \frac{K_m}{R_a + sL_a + Z_e(s)} \quad (1)$$

with the equivalent network of Figure 2(b). The right-hand side of equation (1) can be separated into two parts. The first part, $b_m s + c_m$, is the inertance and damper of the mechatronic network. The second part, $K_m/(R_a + sL_a + Z_e(s))$, can be regarded as the admittance of the electrical circuits of the mechatronic network, where $K_m, R_a,$ and L_a are the motor parameters and $Z_e(s)$ represents the impedance of the connected electrical circuit. Note that the electrical circuit $Z_e(s)$ can be switched at different operating conditions.[9]

We consider seven basic suspension layouts, as illustrated in Figure 3, where F represents the suspension force and v is the relative velocity between two terminals, to discuss the improvement of system stability by inerters. S1 is the conventional suspension. S2 and S3 are the basic parallel and serial arrangements with inerters, respectively. MS1 is a parallel arrangement with the mechatronic network, and MS2–MS4 are the serial arrangements with the mechatronic network. Note that these suspension layouts represent basic element arrangements. More complex layouts are possible by considering the general system impedance and network synthesis, as shown in previous studies.[15–17]

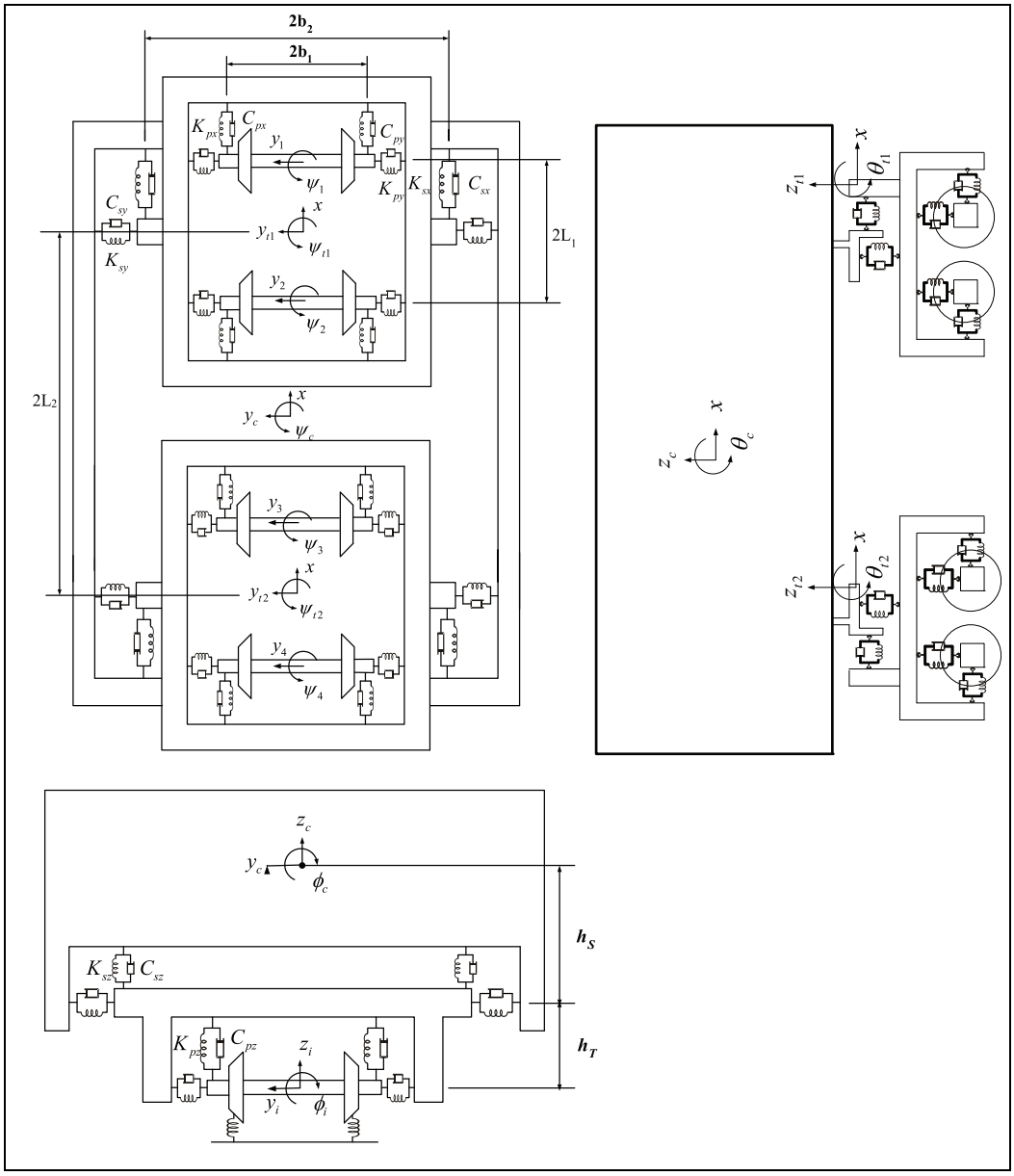

Figure 1. The 31-DOF full-train model.[12]

Table 1. The 31-DOFs of a full-train model.

Component	Type of motion				
	Lateral	Vertical	Roll	Yaw	Pitch
Car body	y_c	z_c	ϕ_c	ψ_c	θ_c
Bogie 1	y_{t1}	z_{t1}	ϕ_{t1}	ψ_{t1}	θ_{t1}
Bogie 2	y_{t2}	z_{t2}	ϕ_{t2}	ψ_{t2}	θ_{t2}
Wheel-set 1	y_1	z_1	ϕ_1	ψ_1	
Wheel-set 2	y_2	z_2	ϕ_2	ψ_2	
Wheel-set 3	y_3	z_3	ϕ_3	ψ_3	
Wheel-set 4	y_4	z_4	ϕ_4	ψ_4	

Table 2. Parameters of the 31 DOF full-train model.[13,14]

Parameters	Symbol	Unit	Default
Car body mass	m_c	kg	8041.3
Bogie mass	m_t	kg	350.26
Wheel-set mass	m_w	kg	1117.9
Roll moment of the inertia of the car body	I_{cx}	kg m^2	31,931
Pitch moment of the inertia of the car body	I_{cy}	kg m^2	386,009
Yaw moment of the inertia of the car body	I_{cz}	kg m^2	357,603
Roll moment of the inertia of the bogie	I_{tx}	kg m^2	118
Pitch moment of the inertia of the bogie	I_{ty}	kg m^2	668
Yaw moment of the inertia of the bogie	I_{tz}	kg m^2	784
Roll moment of the inertia of the wheel-set	I_{wx}	kg m^2	608.1
Spin moment of the inertia of the wheel-set	I_{wy}	kg m^2	72
Yaw moment of the inertia of the wheel-set	I_{wz}	kg m^2	608.1
Nominal wheel-set rolling radius	r_0	m	0.43
Half of the track gauge	a	m	0.7175
Wheel conicity	λ		0.05
Half of the primary longitudinal suspension arm	b_1	m	1
Half of the secondary longitudinal suspension arm	b_2	m	1.29
Half of the primary lateral suspension arm	L_1	m	1.39
Vertical distance from the wheel-set center of the gravity to the secondary suspension	h_T	m	0.47
Vertical distance from the bogie center of the gravity to the car body center of the gravity	h_S	m	1.2
Longitudinal stiffness of primary suspension	K_{px}	N/m	9×105
Lateral stiffness of primary suspension	K_{py}	N/m	3.9×105
Vertical stiffness of primary suspension	K_{pz}	N/m	4.32×105
Longitudinal damping of primary suspension	C_{px}	Ns/m	1×104
Lateral damping of primary suspension	C_{py}	Ns/m	1×104
Vertical damping of primary suspension	C_{pz}	Ns/m	3×104
Longitudinal stiffness of secondary suspension	K_{sx}	N/m	4.5×103
Lateral stiffness of secondary suspension	K_{sy}	N/m	4.5×103
Vertical stiffness of secondary suspension	K_{sz}	N/m	4.5×105
Longitudinal damping of secondary suspension	C_{sx}	Ns/m	9×104
Lateral damping of secondary suspension	C_{sy}	Ns/m	1.8×103
Vertical damping of secondary suspension	C_{sz}	Ns/m	4×103
Simulate vertical stiffness between wheel-set and rail	K_w	N/m	1×106
Lateral creep force coefficient	f_{11}	N	2.212×106
Lateral/spin creep force coefficient	f_{12}	N m^2	3120
Spin creep force coefficient	f_{22}	N	16
Longitudinal creep force coefficient	f_{33}	N	2.563×106
Axle load	W	N	3.2×104

Stability analysis: the critical speed V_{cr}

We now discuss the benefits of inerters in improving the stability of the full-train model. The stability of trains is dominated by the hunting phenomenon, which is caused by the oscillations of the wheel-sets due to the radius variation between the inner and outer sides of wheels. When the train exceeds a critical speed, the hunting motion becomes severe, so that the train could become unstable and run off the tracks.[18] Therefore, we will investigate how the critical speed can be improved by the proposed inerter layouts, especially the mechatronic networks.

The critical speed V_{cr} was defined as[9] the maximum speed V such that all the system eigenvalues $\lambda_i(A_H)$ are located at the left half plane (LHP) if $V < V_{cr}$. That is

$$V_{cr} \equiv \sup\{V_0 | \mathrm{Re}(\lambda_i(A_H)) < 0, \forall i, \text{if} V < V_0\}$$

where A_H is the system matrix of the full-train model. Note that we use the linearized model to analyze the critical speed, because the nonlinear model is very complicated for stability, performance analyses, and optimization. It was shown in Wang et al. (section 3.5)[9] that the nonlinear train models have similar dynamic behaviors to the linear models. Therefore, in this article, we use the linear models for analyses and optimization.

Improvement of V_{cr} by inerter layouts at individual suspension locations

We replace the parallel spring–damper struts of Figure 1 by the proposed inerter layouts and apply the parameters of Table 2. We fix the spring stiffness and optimize other suspension parameters for the critical speed. In addition, we limit the damping rates to less than 100 kNs/m and inertances to less than 5000 kg for practical implementation, and use the following motor constants: $R_a = 2.3\,\Omega$, $L_a = 0.7$ mH, and $K_m = 70560$ VNs/A/m from Wang and Chan[5] for the

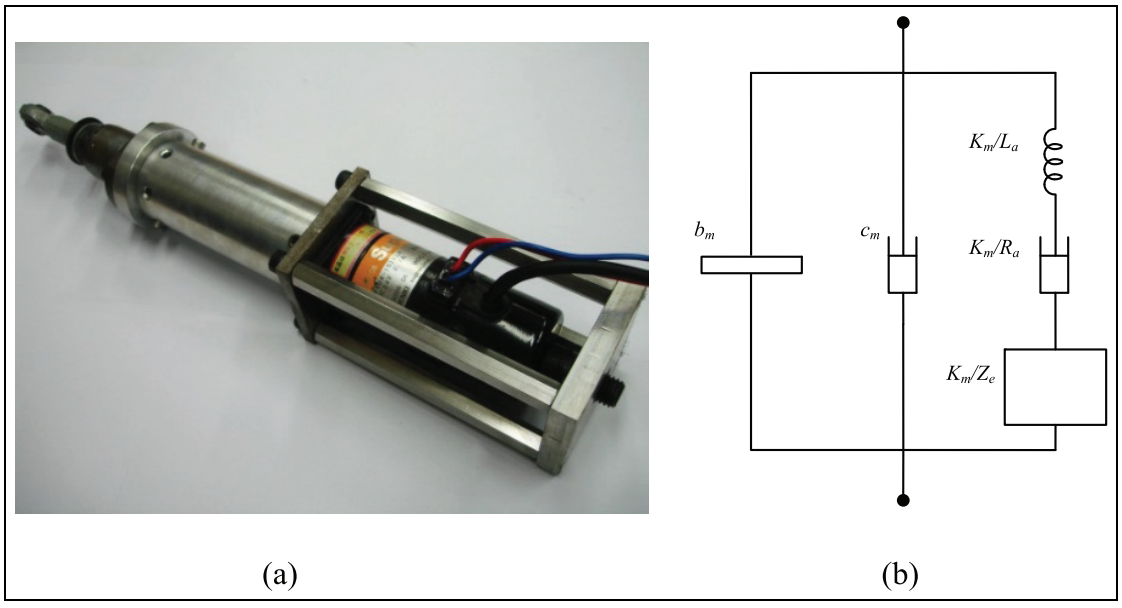

Figure 2. Mechatronic network:[5] (a) a prototype and (b) the network representation.

$$Q_{px}: c_m^{px} = 0\text{Ns}/m, \quad b_m^{px} = 0\text{kg}, \quad Z_e^{px} = \frac{3.522\times10^6 s^2 + 2.382\times10^6 s + 4.887\times10^6}{s^2 + 9.972\times10^6 s + 6.744\times10^6}$$

$$Q_{py}: c_m^{py} = 259\text{Ns}/m, \quad b_m^{py} = 1559\text{kg}, \quad Z_e^{py} = \frac{5.199\times10^6 s^2 + 5.432\times10^6 s + 6.495\times10^6}{s^2 + 1.562\times10^5 s + 2601}$$

$$Q_{pz}: c_m^{pz} = 5616\text{Ns}/m, \quad b_m^{pz} = 2512\text{kg}, \quad Z_e^{pz} = \frac{5.531\times10^6 s^2 + 1.133\times10^6 s + 2.949\times10^6}{s^2 + 1.359\times10^4 s + 2780}$$

$$Q_{sx}: c_m^{sx} = 83345\text{Ns}/m, \quad b_m^{sx} = 4999\text{kg}, \quad Z_e^{sx} = \frac{s^2 + 9.724\times10^6 s + 2.498\times10^6}{2.477\times10^5 s^2 + 6.389\times10^4 s + 4.472\times10^6}$$

$$Q_{sy}: c_m^{sy} = 7557\text{Ns}/m, \quad b_m^{sy} = 7\text{kg}, \quad Z_e^{sy} = \frac{180.917 s^2 + 1.699\times10^6 s + 5.040\times10^4}{s^2 + 1.054\times10^3 s + 9.891\times10^6}$$

$$Q_{sz}: c_m^{sz} = 519\text{Ns}/m, \quad b_m^{sz} = 3474\text{kg}, \quad Z_e^{sz} = \frac{1.251\times10^5 s^2 + 1.218\times10^6 s + 7.36\times10^6}{s^2 + 2.998\times10^4 s + 2.918\times10^5}$$

mechatronic inerter layouts. The optimization results are shown in Table 3. First, the critical speed can be significantly improved by implementing S2 at Q_{py} (8.00%), Q_{pz} (16.12%), Q_{sx} (26.64%), or Q_{sz} (21.63%) with the following suspension parameters

$$Q_{py}: C_{py} = 0\,\text{Ns}/m, \quad b_{py} = 1600\,\text{kg}$$
$$Q_{pz}: C_{pz} = 4600\,\text{Ns}/m, \quad b_{pz} = 2600\,\text{kg}$$
$$Q_{sx}: C_{sx} = 100000\,\text{Ns}/m, \quad b_{sx} = 5000\,\text{kg}$$
$$Q_{sz}: C_{sz} = 0\,\text{Ns}/m, \quad b_{sz} = 3600\,\text{kg}$$

Second, S3 has less influence on the critical speed because the serial layout tends to have more benefits for stiff systems, but the train suspensions are relatively soft.[2] Finally, the critical speed can be further improved by mechatronic networks, especially MS1, with the following suspension settings

Improvement of V_{cr} by inerter layouts at all suspension locations

From Table 3, we note that the critical speed can be significantly improved by the mechanical inerter layout (S2) and the mechatronic inerter network (MS1). Therefore, we now apply S2 and MS1 to all six suspension locations to further improve the critical speed. Because the numbers of adjustable parameters are 12 for S2 and 42 for MS1, we applied the particle swarm optimization (PSO) method[19] to achieve the maximum critical speed. The results are illustrated in Table 4, where the critical speed by S1 might be increased to 1413 km/h by optimizing the corresponding damper settings. In addition, the critical speed can be theoretically further improved to 2846 and 3754 km/h by S2 and MS1, respectively. Note that these speeds might not be practical because the inerter cannot be implemented on

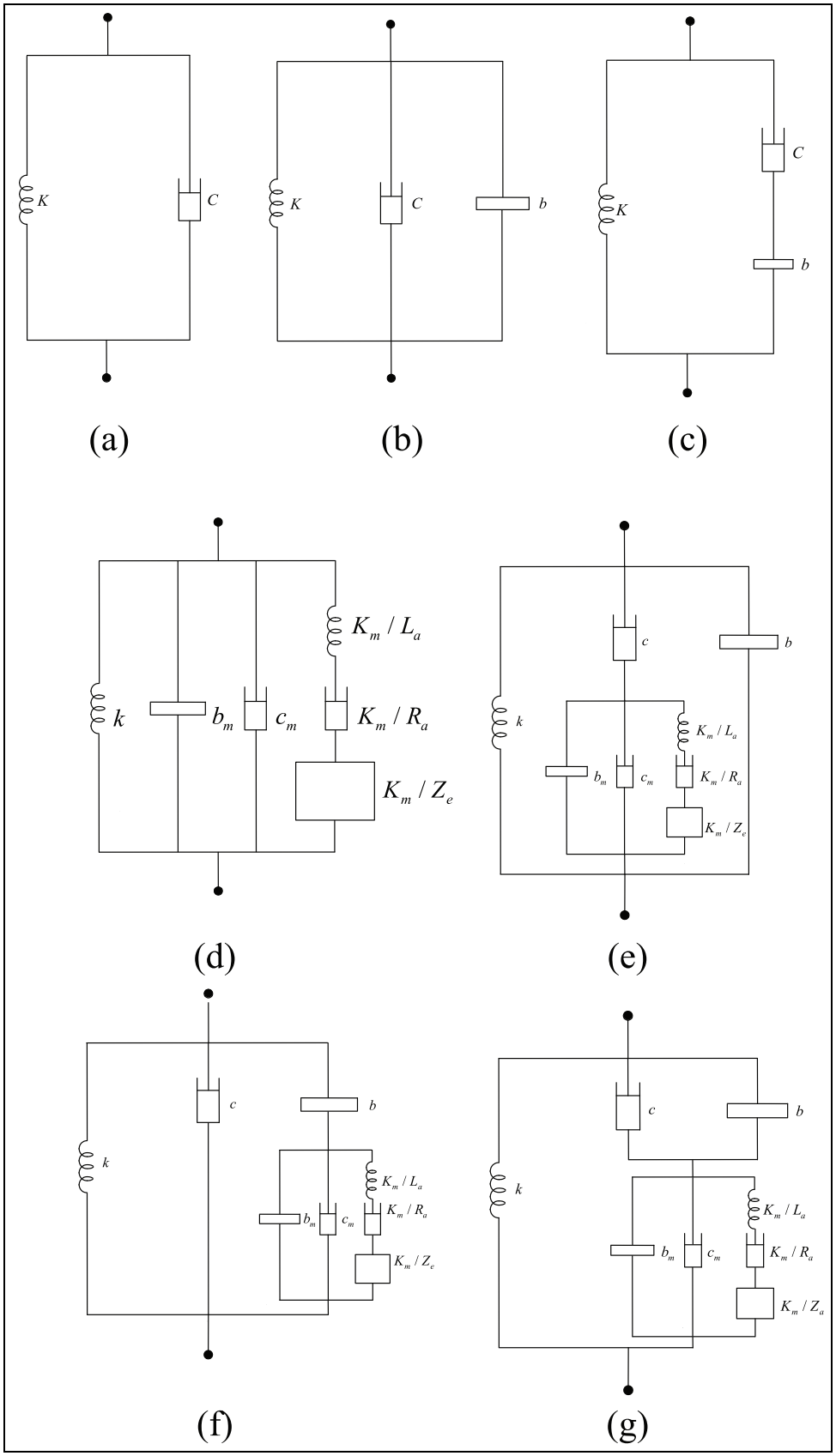

Figure 3. Seven suspension layouts—(a) S1: $\frac{F}{v} = C + \frac{K}{s}$, (b) S2: $\frac{F}{v} = bs + C + \frac{K}{s}$, (c) S3: $\frac{F}{v} = \frac{bCs}{bs + C} + \frac{K}{s}$, (d) MS1: $\frac{F}{v} = \left(\frac{k}{s} + Y_{ms}\right)$, (e) MS2: $\frac{F}{v} = \left(\frac{k}{s} + bs + \frac{cY_{ms}}{c + Y_{ms}}\right)$, (f) MS3: $\frac{F}{v} = \left(\frac{k}{s} + c + \frac{bsY_{ms}}{bs + Y_{ms}}\right)$, and (g) MS4: $\frac{F}{v} = \left(\frac{k}{s} + \frac{(bs + c)Y_{ms}}{bs + c + Y_{ms}}\right)$.

Table 3. Critical speed (km/h) by individual suspension layouts.

	Q_{px}	Q_{py}	Q_{pz}	Q_{sx}	Q_{sy}	Q_{sz}
S1	325	300	304	304	342	319
S2	325	**324**	**353**	**385**	342	**388**
S3	325	307	314	197	325	322
MS1	**347**	**326**	**356**	**414**	**596**	**395**
MS2	330	326	356	258	502	394
MS3	346	326	347	367	483	331
MS4	346	325	354	265	535	330

Note: The bold values are used to specify that they are the optimal in all layouts (or the simple layouts S1~S3).

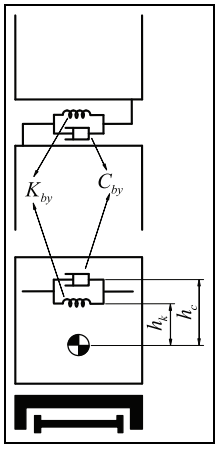

Figure 4. Modeling of restriction between car bodies.[20]

all suspension struts and system performance needs to be considered as well. That is, the design achieves good stability but might result in very poor performance, such as passenger comfort. We will discuss how the improvement will be influenced by connecting train cars and by considering performance in the next section.

Connected multi-car train model

This section extends the discussion to connected multi-car trains, because trains are normally connected in transportation application. The multi-car train model is developed by connecting the single-car trains via parallel spring and damper. We will discuss how the number of connected cars influences system stability and performance. The junction of cars can be represented as shown in Figure 4, where the cars are connected by an equivalent lateral spring with $K_{by} = 20\,\text{kN/m}$ located at $h_k = 0.75\,\text{m}$ and an equivalent lateral damper with $C_{by} = 50\,\text{kNs/m}$ located at $h_c = 1.5\,\text{m}$ above the center of gravity of the car body.[20]

In section "The 31-DOF full-train model," we built the single-car train model using AutoSim. However, we cannot connect more than two cars together in AutoSim because of its element limitation. Therefore, we use another multi-body package, called SimMechanics, to build the connected multi-car train model and compare it with the hand-derived model for verification. First, we derive the dynamic equations of a 12-car train model with 372 DOFs, as illustrated in Appendix 3, and obtain the linearized model, $\bar{G}_H$, as follows

$$\bar{G}_H = \left[\begin{array}{c|c} \bar{A}_H & \bar{B}_H \\ \hline \bar{C}_H & \bar{D}_H \end{array}\right] = \begin{cases} \dot{x} = \bar{A}_H x + \bar{B}_H u \\ y = \bar{C}_H x + \bar{D}_H u \end{cases}$$

Second, we construct the 12-car train model in SimMechanics, as shown in Appendix 4, and obtain the linearized model, $\bar{G}_S$, as follows

$$\bar{G}_S = \left[\begin{array}{c|c} \bar{A}_S & \bar{B}_S \\ \hline \bar{C}_S & \bar{D}_S \end{array}\right] = \begin{cases} \dot{x} = \bar{A}_S x + \bar{B}_S u \\ y = \bar{C}_S x + \bar{D}_S u \end{cases}$$

For model verification, we compare the system matrices, $\bar{A}_H$ and $\bar{A}_S$, and confirm that their elements, eigenvalues, and singular values are the same. Therefore, we can use the SimMechanics model to discuss how the number of cars would influence the system performance and stability.

Influences on the critical speed by the number of cars

We note from Table 4 that the critical speed of a single-car train can be significantly improved by inerter layouts S2 and MS1. Now, we will discuss how the improvement is affected by the number of connected cars. Applying the parameters of Table 4, the critical speed of multi-car trains is shown in Figure 5, where the critical speed is reduced as the number of connected cars increases. For example, the critical speed is dropped from 2846 km/h (1car) to 1727.7 km/h (12 cars) using S2, and from 3754 km/h (1car) to 1179.4 km/h (12 cars) using MS1.

Impacts on the performance

We now discuss the improvement of system performance, such as settling time and passenger comfort, using the inerter layouts. The results illustrate the compromises made in suspension settings between system stability and performance. First, the settling time is

Table 4. Optimization of the critical speed by S2 and MS1 at all suspension locations.

Layout	Location	Suspension parameters
S1 (V_{cr} = 1413km/h)	Q_{px}	C_{px} = 0 Ns/m
	Q_{py}	C_{py} = 2403 Ns/m
	Q_{pz}	C_{pz} = 100,000 Ns/m
	Q_{sx}	C_{sx} = 100,000 Ns/m
	Q_{sy}	C_{sy} = 19,937 Ns/m
	Q_{sz}	C_{sz} = 100,000 Ns/m
S2 (V_{cr} = 2846km/h)	Q_{px}	$C_{px} = 450Ns/m, \quad b_{px} = 81kg$
	Q_{py}	$C_{py} = 3738Ns/m, \quad b_{py} = 971kg$
	Q_{pz}	$C_{pz} = 100,000Ns/m, \quad b_{pz} = 5000kg$
	Q_{sx}	$C_{sx} = 100,000Ns/m, \quad b_{sx} = 0kg$
	Q_{sy}	$C_{sy} = 13,851Ns/m, \quad b_{sy} = 0kg$
	Q_{sz}	$C_{sz} = 100,000Ns/m, \quad b_{sz} = 5000kg$
MS1 (V_{cr} = 3754km/h)	Q_{px}	$c_m^{px} = 111.2Ns/m, \quad b_m^{px} = 0.4kg$
		$Z_e^{px} = \frac{4.335\times10^5 s^2 + 1.064\times10^6 s + 3.222\times10^5}{s^2 + 2.034\times10^6 s + 3.698\times10^6}$
	Q_{py}	$c_m^{py} = 47.4Ns/m, \quad b_m^{py} = 1628.8kg$
		$Z_e^{py} = \frac{985.579s^2 + 532.446s + 2.158\times10^6}{s^2 + 1.78\times10^5 s + 9.784\times10^4}$
	Q_{pz}	$c_m^{pz} = 99987.9Ns/m, \quad b_m^{pz} = 4999.5kg$
		$Z_e^{pz} = \frac{1397.327s^2 + 4.786\times10^4 s + 1.308\times10^7}{s^2 + 3.47\times10^5 s + 1.184\times10^7}$
	Q_{sx}	$c_m^{sx} = 99563.7Ns/m, \quad b_m^{sx} = 0kg$
		$Z_e^{sx} = \frac{190.294s^2 + 158.817s + 1.676\times10^6}{s^2 + 7.76\times10^5 s + 6.56\times10^5}$
	Q_{sy}	$c_m^{sy} = 8.8Ns/m, \quad b_m^{sy} = 4.7kg$
		$Z_e^{sy} = \frac{2.337\times10^4 s^2 + 9.938\times10^5 s + 5.456\times10^6}{s^2 + 5.521\times10^4 s + 2.058\times10^6}$
	Q_{sz}	$c_m^{sz} = 99670.5Ns/m, \quad b_m^{sz} = 4999.9kg$
		$Z_e^{sz} = \frac{1.605\times10^5 s^2 + 2.176\times10^6 s + 5.989\times10^6}{s^2 + 4.925\times10^4 s + 4.32\times10^5}$

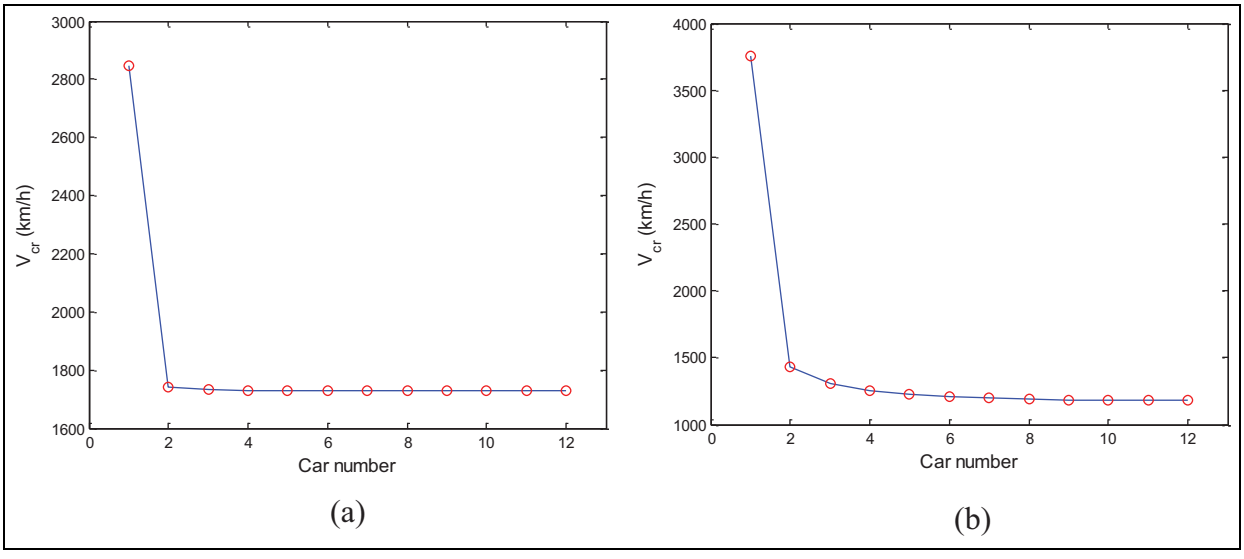

Figure 5. Critical speed versus the number of connected cars: (a) S2 and (b) MS1.

defined as the time required for the system responses $y(t)$ to remain within 2% of the maximum value in the impulse response[9,21]

$$t_s = \min\{T_0 | |y(t) - y(\infty)| < 0.02|y|_{\max}, \text{for } t > T_0\}$$

Because the settling time significantly increases when the forward velocity is greater than 1500 km/h, we define the following cost function for settling-time optimization

$$J_0 = \sum_{i=1}^{10} \frac{t_s(V_i)}{10} \quad (2)$$

That is, we adjust the suspension parameters to reduce the settling time at 10 different velocities. We set the velocities as linearly spaced between 1500 and 0.9 V_{cr} (e.g. V_i = 1500, 1618, …, 2561 km/h for S2).

Another important performance index, called *the Passenger comfort*, is defined as the 2-norm of the transfer function from the road profile to the vertical velocity of the car[9]

$$J_1 = \|T_{z_r \to \dot{z}_c}\|_2 = \|sT_{z_r \to z_c}\|_2$$

where $T_{z_r \to \dot{z}_c}$ is the transfer function from the road displacement z_r to the vertical velocity of the car body $\dot{z}_c$, and $\|T\|_2$ is the H_2-nom of the system T. For example, J_1 = 12.4934 using the default suspensions of Table 2. We place S2 and MS1 at all suspensions and optimize the suspension settings for the critical speed, settling time, and passenger comfort simultaneously. For S2, we follow the same optimization procedures used previously (see Table 8 in Wang et al.[9]). That is, we optimize Q_z for J_1, and Q_x, Q_y for V_{cr} by iterations until any further improvement is negligible. We then use Q_x and Q_y for settling-time optimization using equation (2). For MS1, we use the following equations for further improvement

$$J = \alpha \frac{J_0}{J_0^{S2}} + (1 - \alpha) \frac{J_1}{J_1^{S2}}$$

where α = 0.5. The optimization for a single-car train is illustrated in Table 5. First, using S2, the critical speed V_{cr}^{S2} = 606 km/h, which is greatly reduced from its optimal critical speed V_{cr} = 2846 km/h (see Table 4). However, the settling time is also greatly reduced from 89.2210 s to J_0^{S2} = 9.7802s, with the corresponding passenger comfort J_1^{S2} = 7.1107. That is, the suspension settings are the compromises between system stability and performance. Second, for MS1, the critical speed, V_{cr}^{MS1} = 1675km/h, settling time, J_0^{MS1} = 3.1969 s, and

Table 5. Optimization of V_{cr}, J_0, and J_1 using all suspension locations.

Layout	Location	Suspension parameters
S2 (V_{cr} = 606km/h)	Q_{px}	$C_{px} = 2834Ns/m, \quad b_{px} = 0.4kg$
(J_0 = 9.7802s)	Q_{py}	$C_{py} = 627Ns/m, \quad b_{py} = 632kg$
(J_1 = 7.1107)	Q_{pz}	$C_{pz} = 18467Ns/m, \quad b_{pz} = 2207kg$
	Q_{sx}	$C_{sx} = 99289Ns/m, \quad b_{sx} = 4991kg$
	Q_{sy}	$C_{sy} = 5463Ns/m, \quad b_{sy} = 22kg$
	Q_{sz}	$C_{sz} = 902Ns/m, \quad b_{sz} = 296kg$
MS1 (V_{cr} = 1675km/h)	Q_{px}	$c_m^{px} = 8182.7Ns/m, \quad b_m^{px} = 139.8kg$
(J_0 = 3.1969s)		
(J_1 = 3.0523)		$Z_e^{px} = \frac{2.983\times10^7 s^2 + 3.072\times10^7 s + 6.090\times10^7}{s^2 + 7.607\times10^7 s + 7.165\times10^7}$
	Q_{py}	$c_m^{py} = 95853.8Ns/m, \quad b_m^{py} = 224.8kg$
		$Z_e^{py} = \frac{3.469\times10^7 s^2 + 8.647\times10^7 s + 6.120\times10^7}{s^2 + 9.686\times10^7 s + 9.996\times10^7}$
	Q_{pz}	$c_m^{pz} = 97248.2Ns/m, \quad b_m^{pz} = 49.5kg$
		$Z_e^{pz} = \frac{8.707\times10^7 s^2 + 8.831\times10^7 s + 4.703\times10^6}{s^2 + 9.862\times10^7 s + 9.999\times10^7}$
	Q_{sx}	$c_m^{sx} = 99417.9Ns/m, \quad b_m^{sx} = 634.1kg$
		$Z_e^{sx} = \frac{2.725\times10^7 s^2 + 1.987\times10^7 s + 8.269\times10^6}{s^2 + 9.909\times10^7 s + 7.219\times10^7}$
	Q_{sy}	$c_m^{sy} = 9362.4Ns/m, \quad b_m^{sy} = 9.6kg$
		$Z_e^{sy} = \frac{9.548\times10^6 s^2 + 2.639\times10^7 s + 1.606\times10^7}{s^2 + 2.674\times10^7 s + 4.186\times10^7}$
	Q_{sz}	$c_m^{sz} = 95693.1Ns/m, \quad b_m^{sz} = 2724kg$
		$Z_e^{sz} = \frac{7.251\times10^6 s^2 + 1.838\times10^7 s + 7.179\times10^6}{s^2 + 6.448\times10^7 s + 6.148\times10^7}$

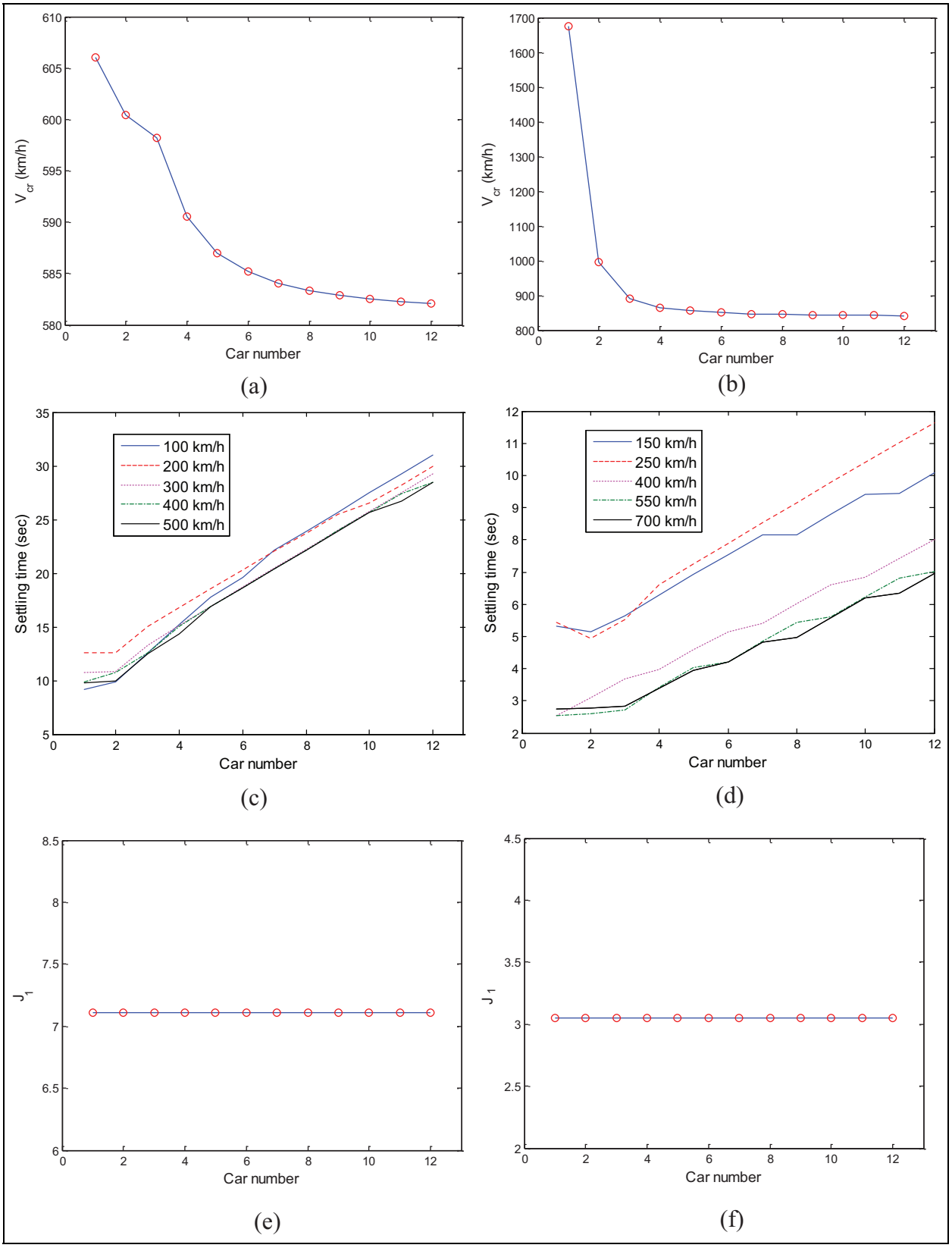

Figure 6. Impacts of car numbers on stability and performance: (a) critical speed by S2, (b) critical speed by MS1, (c) settling time by S2, (d) settling time by MS1, (e) passenger comfort by S2, and (f) passenger comfort by MS1.

the passenger comfort, $J_1^{MS1} = 3.0523$, are all significantly improved by the mechatronic network. Note that the electrical circuit Z_e of MS1 can be switched for further improvement of the settling time at different velocities, as illustrated in Wang et al.[9]

We now further discuss the influences of connecting cars on system stability and performance. Using the parameters of Table 5, the impacts of the number of cars on the critical speed, settling time, and passenger comfort are shown in Figure 6. First, the critical speed drops from 606 km/h (1 car) to 582.1 km/h (12 cars) using S2 (see Figure 6(a)), and from 1675.9 km/h (1 car) to 841.7 km/h (12 cars) using MS1 (see Figure 6(b)). Although MS1 has a larger degradation (about 50%) than S2 (about 4%), its achievable critical speed is still much higher than S2. Second, the settling time tends to increase when the number of cars increases. For example, at a forward speed of 400 km/h, the settling time increases from 9.9 s (1 car) to 28.5 s (12 cars) using S2 (see Figure 6(c)), and from 2.5 s (1 car) to 8.0 s (12 cars) using MS1 (see Figure 6(d)). Finally, the passenger comfort is shown to be significantly improved by the inerter. However, it is independent of the car numbers (see Figure 6(e) and (f)), because only the vertical suspensions (i.e. Q_{pz} and Q_{sz}) can influence the passenger comfort J_1, while the connecting spring–damper is set horizontally and does not change the vertical dynamics of the linear models. Note that we only consider these three indexes to demonstrate the benefits of inerters. Other performance[10] might also be evaluated in the similar way.

Network synthesis

The mechatronic network is shown to improve stability and performance of the train systems. In this section, we will show how to realize the designed impedance Z_e by the network synthesis methods. For example, section "The 31-DOF full-train model" illustrates that the critical speed is increased to $V_{cr} = 596$km/h by employing MS1 at Q_{sy} with the following circuit (see Table 3)

$$Z_e^{sy} = \frac{180.917s^2 + 1.699 \times 10^6 s + 5.040 \times 10^4}{s^2 + 1.054 \times 10^3 s + 9.891 \times 10^6}$$

This circuit can be realized by the method in Jiang and Smith[17] to be a five-element circuit of Figure 7 with the following parameters

$$\begin{aligned} &C = 5.8875 \times 10^{-7}\text{F}, \quad L = 0.1717\text{H}, \\ &R_1 = 5.0954 \times 10^{-3}\Omega, \quad R_2 = 1.8091 \times 10^{2}\Omega, \\ &R_3 = 1.7345 \times 10^{6}\Omega \end{aligned} \tag{3}$$

We will now discuss the nonlinearities of the mechatronic network and construct experiments for verification. The nonlinearity of the mechatronic network

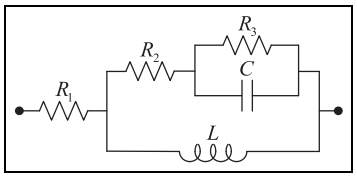

Figure 7. Network realization of Z_e^{sy}.[17]

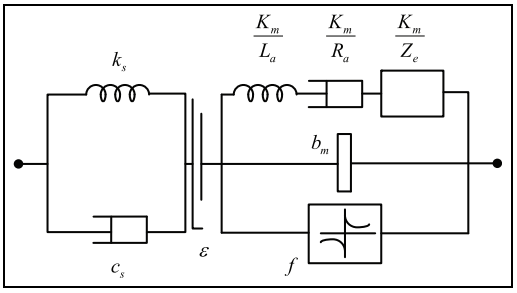

Figure 8. Nonlinear mechatronic network model.

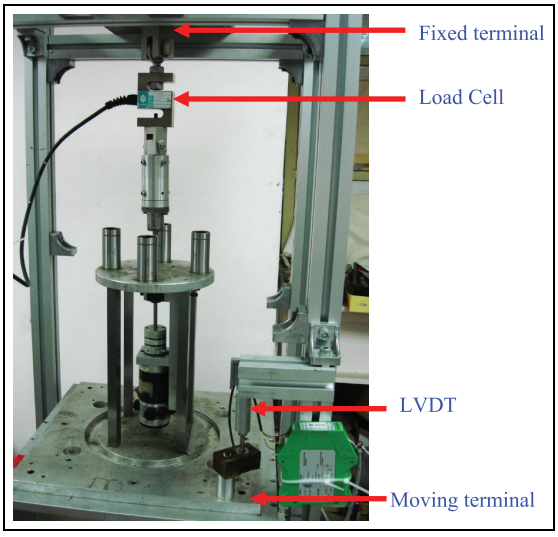

Figure 9. Testing platform.

includes the elastic effects, backlash, and friction, as shown in Figure 8, where k_s and c_s are the elasticity and viscous damping, respectively, ε is the backlash of the ball-screw set, and f represents the friction force.[5,9] The friction is depicted by the following Stribeck friction–Tustin model[5]

$$f(v) = F_s(\alpha + (1-\alpha)e^{-|v|/v_s}) \cdot \text{sgn}(v) + F_v v$$

where F_c and F_s are the Coulomb friction and static friction, respectively, $\alpha = F_c/F_s$ with $0 < \alpha \leq 1$, v_s is the Stribeck velocity, and F_v is the viscous damping.

We design a vertical platform, as illustrated in Figure 9, to identify the system parameters. First, we set the circuit impedance $Z_e = \infty$ and generated

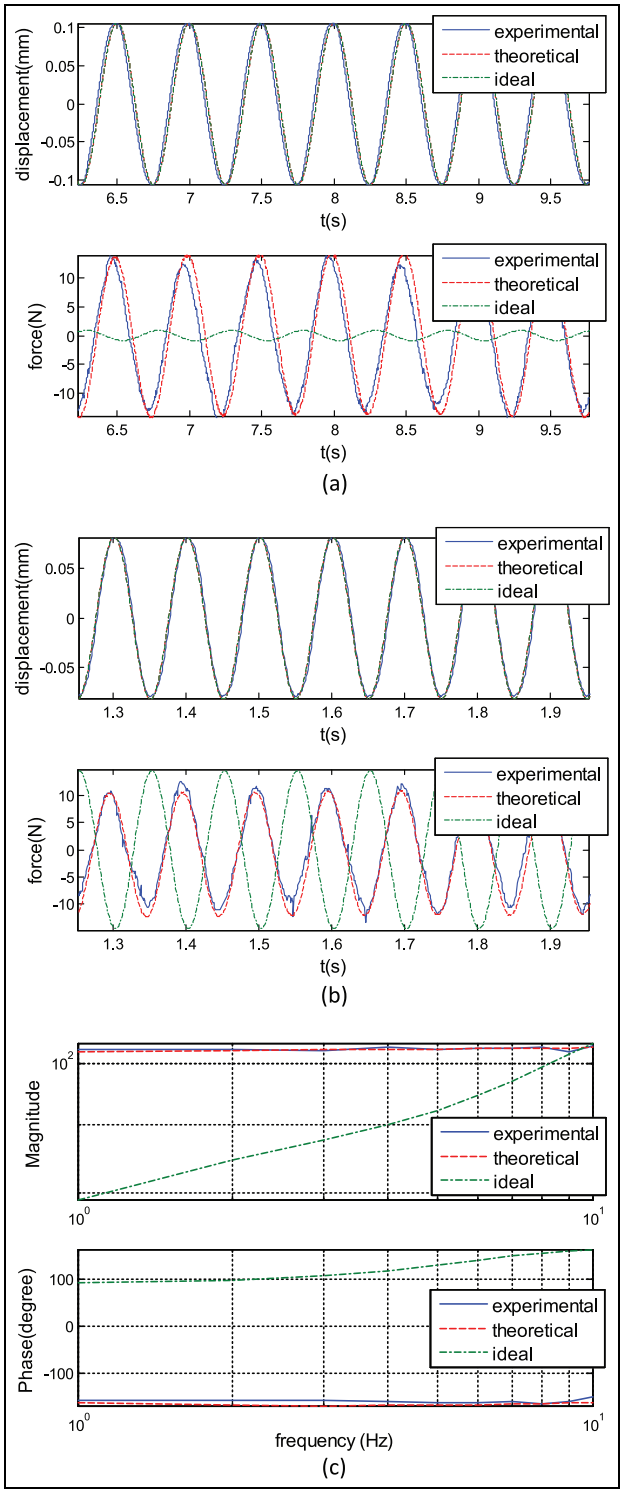

Figure 10. Responses of the models: (a) time responses (2 Hz), (b) time responses (10 Hz), and (c) frequency responses.

sinusoidal displacement input to drive the moving terminal. We then measured the reacting force and the strut displacement by an S-type load cell and the linear variable differential transformer (LVDT), respectively. Subsequently, we minimized the root-mean-square error between theoretical and experimental forces to obtain the system parameters as follows: $F_s = 16.89\,\text{N}$, $\alpha = 0.8958\,\text{m}$, $v_s = 15.46\,\text{mm/s}$, $F_v = 0.0016\,\text{Ns/m}$, $b_m = 45.13\,\text{kg}$, $k_s = 133.59\,\text{kN/m}$, $c_s = 726.76\,\text{Ns/m}$, and $\varepsilon = 0.1\,\mu\text{m}$.

We constructed Z_e^{sy} by the five-element circuit of Figure 7 with the parameters of equation (3), and connected it to the PMEM for experimental tests. The time and the frequency responses are illustrated in Figure 10. The "ideal" and "theoretical" represent the simulation results using the linear (Figure 2(b)) and nonlinear (Figure 8) models, respectively, whereas "experimental" represents the responses obtained from the experimental data. The results indicate that an agreement between the nonlinear theoretical responses and the experimental data, that is, the nonlinear model can accurately describe the dynamics of the mechatronic network.

Conclusion

This article has discussed the benefits of inerters for a connected multi-car train model. First, we built a 31-DOF full-train model by hand derivation and AutoSim, and showed the improvements in critical speed by the inerter. Second, we derived a connected multi-car train model by SimMechanics for verification and demonstrated that car connection can decrease the critical speed. Furthermore, we extended the discussion to performance and showed that connecting cars can increase the settling time, but have no influence on the passenger comfort. Finally, we realized one optimal electrical circuit of the mechatronic inerter by network syntheses and conducted experimental verification. Based on the results, the inerters are deemed effective in improving the stability and performance of the connected multi-car train systems. In the future, the results can be applied to design suspensions for different types of train models, for example, the passenger rail vehicle in Hirotsu et al.[14] that has much higher mass and inertia. Furthermore, we considered the model nonlinearities and discussed their effects on system performance to estimate the practical applications. Finally, experiments should be conducted to verify the effectiveness of the inerter on train systems.

Declaration of conflicting interests

The author(s) declared no potential conflicts of interest with respect to the research, authorship, and/or publication of this article.

Funding

The author(s) disclosed receipt of the following financial support for the research, authorship, and/or publication of this article: This work was supported in part by the

National Science Council of Taiwan under grant no. 95-2218-E-002-030.

References

1. Smith MC. Synthesis of mechanical networks: the inerter. *IEEE T Automat Contr* 2002; 47: 1648–1662.
2. Smith MC and Wang FC. Performance benefits in passive vehicle suspensions employing inerters. *Vehicle Syst Dyn* 2004; 42: 235–257.
3. Wang FC and Sue WJ. The impact of inerter nonlinearities on vehicle suspension control. *Vehicle Syst Dyn* 2008; 46: 575–595.
4. Wang FC, Hong MF and Lin TC. Designing and testing a hydraulic inerter. *Proc IMechE, Part C: J Mechanical Engineering Science* 2011; 225: 66–72.
5. Wang FC and Chan HA. Vehicle suspensions with a mechatronic network strut. *Vehicle Syst Dyn* 2011; 49: 811–830.
6. Evangelou S, Limebeer DJN, Sharp RS, et al. Mechanical steering compensators for high-performance motorcycles. *J Appl Mech: T ASME* 2007; 74: 332–346.
7. Wang FC, Hong MF and Chen CW. Building suspensions with inerters. *Proc IMechE, Part C: J Mechanical Engineering Science* 2010; 224: 1605–1616.
8. Wang FC and Liao MK. The lateral stability of train suspension systems employing inerters. *Vehicle Syst Dyn* 2010; 48: 619–643.
9. Wang FC, Hsieh MR and Chen HJ. Stability and performance analysis of a full-train system with inerters. *Vehicle Syst Dyn* 2012; 50: 545–571.
10. Jiang JZ, Matamoros-Sanchez AZ, Goodall RM, et al. Passive suspensions incorporating inerters for railway vehicles. *Vehicle Syst Dyn* 2012; 50: 263–276.
11. Ling L, Xiao XB, Xiong JY, et al. A 3D model for coupling dynamics analysis of high-speed train/track system. *J Zhejiang Univ* 2014; 15: 964–983.
12. Fan YT and Wu WF. Stability analysis of railway vehicles and its verification through field test data. *J Chin Inst Eng* 2006; 29: 493–505.
13. Ahmed AKW and Sankar S. Lateral stability behavior of railway freight car system with elasto-damper coupled wheelset: part 2-truck model. *J Mech Transm: T ASME* 1987; 109: 500–507.
14. Hirotsu T, Terada K, Hiraishi M, et al. Simulation of hunting of rail vehicles (the case using a compound circular wheel profile). *JSME Int J III: Vib C* 1990; 56: 2149–2157.
15. Papageorgiou C and Smith MC. Positive real synthesis using matrix inequalities for mechanical networks: application to vehicle suspension. *IEEE T Contr Syst T* 2006; 14: 423–435.
16. Chen MCQ and Smith MC. Restricted complexity network realizations for passive mechanical control. *IEEE T Automat Contr* 2009; 54: 2290–2301.
17. Jiang JZ and Smith MC. Regular positive-real functions and five-element network synthesis for electrical and mechanical networks. *IEEE T Automat Contr* 2011; 56: 1275–1290.
18. Claus H and Schiehlen W. Stability analysis of railways with radial-elastic wheelsets. *Vehicle Syst Dyn* 2002; 37: 453–464.
19. Wang FC and Ko CC. Multivariable robust PID control for a PEMFC system. *Int J Hydrogen Energ* 2010; 35: 10437–10445.
20. Kikko S, Tanifuji K, Sakanoue K, et al. Modeling of aerodynamic force acting in tunnel for analysis of riding comfort in a train. *J Mech Syst Transp Logist* 2008; 1: 31–42.
21. Dorf RC and Bishop RH. *Modern control systems*. Upper Saddle River, NJ: Pearson, 2008.

Appendix 1

The dynamic equations of the 31-DOF train model is available on: http://140.112.14.7/~sic/PaperMaterial/Dynamics_of_a_Train_model.pdf

Appendix 2

The AutoSim codes of the 31-DOF full-train model is available on: http://140.112.14.7/~sic/PaperMaterial/AUTOSIM_CODE_31-DOF_Full-train_Model.html

Appendix 3

The derivation of a 12-car train model is available on: http://140.112.14.7/~sic/PaperMaterial/Derivation_Twelve-car_Train_Model.pdf

Appendix 4

The SimMechanics model of a 12-car train is available on: http://140.112.14.7/~sic/PaperMaterial/SimMechanics_Model_Twelve-car_train.html